Cell Calcium 67 (2017) 31–39

Contents lists available at ScienceDirect

Cell Calcium

journal homepage: www.elsevier.com/locate/ceca

Differential Ca^{2+} mobilization and mast cell degranulation by FcεRI- and GPCR-mediated signaling

Ying-Chi Chen[a], Yu-Chung Chang[a], Heng-Ai Chang[b], Yu-Shan Lin[b], Chiung-Wen Tsao[c], Meng-Ru Shen[b,d], Wen-Tai Chiu[a,b,e,*]

[a] Department of Biomedical Engineering, National Cheng Kung University, Tainan 701, Taiwan
[b] Institute of Basic Medical Sciences, National Cheng Kung University, Tainan 701, Taiwan
[c] Department of Nursing, Chung Hwa University of Medical Technology, Tainan 717, Taiwan
[d] Department of Pharmacology, National Cheng Kung University, Tainan 701, Taiwan
[e] Medical Device Innovation Center, National Cheng Kung University, Tainan 701, Taiwan

ARTICLE INFO

Article history:
Received 14 April 2017
Received in revised form 3 August 2017
Accepted 3 August 2017

Keywords:
Ca^{2+}
TIRFM
Histamine
Degranulation
SOCE
Nile red

ABSTRACT

Mast cells play a primary role in allergic diseases. During an allergic reaction, mast cell activation is initiated by cross-linking IgE-FcεRI complex by multivalent antigen resulting in degranulation. Additionally, G protein-coupled receptors also induce degranulation upon activation. However, the spatio-temporal relationship between Ca^{2+} mobilization and mast cell degranulation is not well understood. We investigated the relationship between oscillations in Ca^{2+} level and mast cell degranulation upon stimulation in rat RBL-2H3 cells. Nile red and Fluo-4 were used as probes for monitoring histamine and intracellular Ca^{2+} levels, respectively. Histamine release and Ca^{2+} oscillations in real-time were monitored using total internal reflection fluorescence microscopy (TIRFM). Mast cell degranulation followed immediately after FcεRI and GPCR-mediated Ca^{2+} increase. FcεRI-induced Ca^{2+} increase was higher and more sustained than that induced by GPCRs. However, no significant difference in mast cell degranulation rates was observed. Although intracellular Ca^{2+} release was both necessary and sufficient for mast cell degranulation, extracellular Ca^{2+} influx enhanced the process. Furthermore, cytosolic Ca^{2+} levels and mast cell degranulation were significantly decreased by downregulation of store-operated Ca^{2+} entry (SOCE) via Orai1 knockdown, 2-aminoethyl diphenylborinate (2-APB) or tubastatin A (TSA) treatment. Collectively, this study has demonstrated the role of Ca^{2+} signaling in regulating histamine degranulation.

1. Introduction

The release of histamine from mast cells is a key event during an allergic response. When allergy-prone people come in contact with an allergen such as pollen or dust mite for the first time, their B cells differentiate into plasma cells, which produce large quantities of antigen-specific IgE. Following this, IgE binds to the mast cells but does not cause an allergic reaction. Upon subsequent attack by the same allergen, IgE stimulates the mast cells to release chemical mediators such as cytokines and histamine [1,2]. These chemical mediators cause the characteristic symptoms of allergy.

The allergic responses are mediated *via* two signaling pathways resulting in mast cell degranulation. One is the IgE-dependent, and the other is the IgE-independent signaling pathway. The IgE-dependent signaling pathway mimics physiological antigen exposure by cross-linking the IgE-FcεRI complexes with the multivalent antigen [3], while the IgE-independent signaling pathway occurs through the activation of G protein-coupled receptors (GPCRs) [4]. The high-affinity immunoglobulin E receptor (FcεRI) expressed on the surface of mast cells [5] is a tetrameric receptor complex consisting of one α, one β, and two γ chains. While the α-chain forms the IgE-binding site, the β-chain amplifies and the γ-chain initiates the downstream signaling pathway, respectively. Cross-linking of the IgE-FcεRI complex by a multivalent antigen initiates the phosphorylation of the immunoreceptor tyrosine-based activation motifs (ITAMs) found in the cytoplasmic β and γ_2 subunits of the FcεRI receptor by Lyn, a Src protein tyrosine kinase, which then leads to the recruitment and activation of another tyrosine kinase, Syk. Syk phosphorylates and activates phospholipase Cγ (PLCγ) tethered to LAT, a transmembrane adaptor molecule. Hydrolysis of phosphatidylinositol 4, 5-bisphosphate (PIP_2) by

* Corresponding author at: Department of Biomedical Engineering, National Cheng Kung University, Tainan, 701, Taiwan.
E-mail address: wtchiu@mail.ncku.edu.tw (W.-T. Chiu).

http://dx.doi.org/10.1016/j.ceca.2017.08.002
0143-4160/

PLCγ produces two second messengers, diacylglycerol (DAG) and inositol 1, 4, 5-trisphosphate (IP_3). IP_3-mediated Ca^{2+} release from the ER and the combination of Ca^{2+} activation of PKC are necessary and sufficient for degranulation of the mast cells [6–8].

In addition to the above, mast cell activation can also be triggered by a large number of polycationic molecules, collectively known as basic secretagogues. These include polyamines like spermine and compound 48/80 (48/80) [9,10], venom peptides like mastoparan, and neurotransmitters such as substance P [11], which cause neurogenic inflammation [12]. The negatively charged sialic acid residues (SIA) present on the mast cell membranes, are thought to assemble the positively charged molecules, such as 48/80, at the cell surface. Following this, the polycationic molecules interact with the GPCRs that are coupled with the $G_{\alpha i}$ family of heterotrimeric G proteins [13,14]. Previous studies have demonstrated that the basic secretagogue signaling pathway induces degranulation in the mast cells by the activation of the heterotrimeric Gα protein ($G_{\alpha i2}$ and $G_{\alpha i3}$), by associating with the $G_{\beta\gamma}$ subunits to stimulate phospholipase Cβ (PLCβ), which results in the release of histamine [12,15,16]. Similar to the activation of PLCγ by the IgE-FcεRI complexes, activation of PLCβ by GPCRs also leads to the hydrolysis of PIP_2 to yield DAG and IP_3.

During exocytosis and release of histamine [17,18], Ca^{2+} plays an important role in the fusion of the secretory vesicles with the plasma membrane [19,20]. Elevation in the intracellular Ca^{2+} level after exposure to the allergens may be due to the ER-releasable fraction and extracellular Ca^{2+} influx. Store-operated Ca^{2+} entry (SOCE) is the major form of extracellular Ca^{2+} influx following depletion of ER Ca^{2+} stores in non-excitable cells, like mast cells. Activation of SOCE is used to refill intracellular Ca^{2+} stores, regulate basal Ca^{2+}, and excute a wide range of Ca^{2+}-associated specialized activities [21]. Activation of both IgE-FcεRI complexes and GPCRs by allergens shares a similar signaling mechanism in inducing ER-releasable Ca^{2+} and SOCE. Stromal interaction molecule 1 (STIM1) is a transmembrane protein, which is localized mainly in the ER and acts as a Ca^{2+} sensor. When STIM1 senses a decrease in the Ca^{2+} concentration in the ER, it translocates to specific ER-plasma membrane junctional regions, where it activates CRACM1 (calcium release-activated calcium modulator 1 or Orai1) and TRPC1 (transient receptor potential canonical 1) channels, enabling extracellular Ca^{2+} influx. Microtubules are essential for translocation of STIM1 to the plasma membrane and its interaction with Orai1 for activation of SOCE [22,23]. Microtubule-associated histone deacetylase 6 (HDAC6) induces the activation of STIM1-mediated SOCE by enhancing the translocation of STIM1 to the plasma membrane. Therefore, SOCE activated in the plasma membrane induces extracellular Ca^{2+} influx and promotes the events related to degranulation [24–26].

Nile red is a fluorescent probe used for the detection of histamine [27,28]. The measurement of histamine is based on a ligand exchange reaction between the former and the iminodiacetic acid ligands in the probe coordinated with Ni^{2+}. Nile red is lipophilic in nature and localizes in the intracellular lipid droplets. It comprises iminodiacetic acid moieties, whose fluorescent properties are known to change upon binding to metal ions like Ni^{2+}. Ni^{2+} bound to the iminodiacetic acid residues acts as a quencher, and strongly quenches the fluorescence of Nile red. When the probe is present in the histamine-containing secretory granules of the mast cells, it preferably coordinates with histamine. Ni^{2+} is preferably exchanged with histamine to form a histamine-Ni^{2+} complex, and Nile red exhibits a stronger fluorescence. Therefore, Nile red is suitable for the real-time monitoring of histamine in living cells [27].

The mast cell degranulation pathway has been popularly studied using the rat basophilic leukemia RBL-2H3 cell line, because of its reliability in the release of histamine upon initiation by IgE-FcεRI complexes and their functional similarity to the primary human basophils and rodent mast cells. IgE-FcεRI complex-mediated and GPCR-activated signaling pathways commonly require the participation of Ca^{2+}. However, the differences between these pathways in Ca^{2+} mobilization and mast cell degranulation have not yet been fully understood. Regular assays for mast cell degranulation, such as β-hexosaminidase release assay, are either single point assays or endpoint assays measuring the cumulative release of mediators. Their limitations regarding single-cell level, real-time and sensitive analysis make them unsuitable for dynamic and high spatiotemporal detection. Kim et al. have demonstrated the temporal relationship between changes in intracellular Ca^{2+} and serotonin secretion at the single-cell level using simultaneous indo-1 photometry and constant potential amperometry, which has a much faster temporal resolution and reveals dynamic changes in living RBL-2H3 cells [29]. In this study, we examined the relationship between Ca^{2+} mobilization and mast cell degranulation after stimulation of two different signaling pathways using total internal reflection fluorescence microscopy (TIRFM) in real-time. We found that Ca^{2+} mobilization from the ER is both necessary and sufficient for the release of histamine. However, extracellular Ca^{2+} promotes, but is not essential for, mast cell degranulation. We also observed that downregulation of SOCE reduces the intracellular Ca^{2+} levels and delays mast cell degranulation and histamine release.

2. Results

The aim of this study was to understand the effect of oscillations in Ca^{2+} level on mast cell degranulation and histamine release through activation of FcεRI and GPCR-mediated signaling pathways in real-time. The RBL-2H3 cell line is routinely used for measuring histamine release in inflammation, allergic responses, and other immunology-related studies. Here, we used TNP-BSA and monoclonal anti-TNP IgE antibody to activate the high-affinity IgE receptor, FcεRI; and 48/80 to activate the GPCRs in rat RBL-2H3 cell line. Degranulation of mast cells occurs during allergic reactions. In order to decrease the noise arising from the non-plasma membrane regions, TIRFM was used to record the fluorescence signals within 50–100 nm range of the glass surface, which includes the basal plasma membrane of the cells. This ensures that the incident light excites the fluorophores near the plasma membrane only.

2.1. Entrapment of nile red-labeled histamine within secretory granules

Nile red is a fluorescent probe for detection of histamine, which displays red fluorescence. Previous studies have reported that when Nile red is present in the secretory granules containing histamine in the mast cells, the ability of Ni^{2+} ions to quench the Nile red fluorescence was suppressed by histamine coordination, resulting in the dissociation of Ni^{2+} from the probe, followed by a drastic increase in the fluorescence of Nile red [27,28]. As shown in Fig. 1A, Nile red-labeled histamine was enclosed within the secretory granules, expressing CD63 as a marker. Additionally, the anti-histamine antibody was also used to ascertain whether Nile red could be used as an effective probe in measuring histamine in the secretory granules of mast cells by immunofluorescence. Our data showed that histamine was localized within the secretory granules (Fig. 1B). The spatial patterns of the Nile red-labeled histamine residues were the same as those observed for the anti-histamine antibody. Therefore, we concluded that Nile red could be used as a valuable tool for observation of the events related to mast cell degranulation.

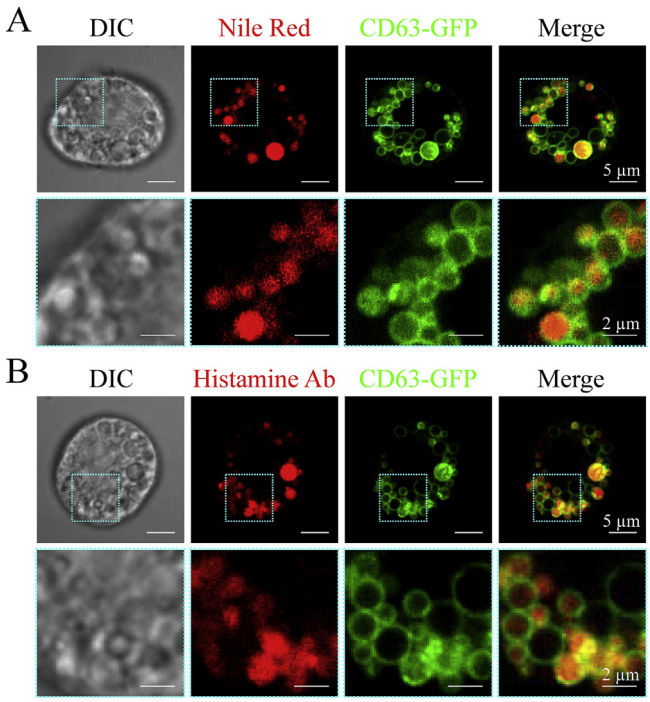

Fig. 1. Visualization of Nile red-labeled histamine enclosed in secretory granules of rat RBL-2H3 cell line. (A) Figure showing the DIC and fluorescence images of Nile red and GFP-tagged CD63 (CD63-GFP) cells (upper panel) using confocal microscopy (scale bar, 5 μm). Nile red and GFP were excited with 543 and 488 nm laser, respectively. The pictures in the lower panel represent magnification of the cyan rectangles in the upper panel (scale bar, 2 μm). (B) Figure showing the DIC and fluorescence images of Alexa 543 and CD63-GFP using confocal microscopy (upper panel). Anti-histamine primary antibody (Histamine Ab) and Alexa fluor 543-conjugated secondary antibody were used to detect endogenous histamine. Alexa fluor 543 and GFP were excited with 543 and 488 nm laser, respectively (scale bars, 5 μm). The pictures in the lower panel represent magnification of the cyan rectangles in the upper panel (scale bar, 1 μm). (For interpretation of the references to colour in this figure legend, the reader is referred to the web version of this article.)

2.2. Elevation in cytosolic Ca^{2+} levels triggers immediate degranulation of mast cells

There exists a strong correlation between mast cell degranulation and Ca^{2+} mobilization. However, the temporal and spatial relationships between the two processes requires further investigation. The Ca^{2+} indicator (Fluo-4) and histamine probe (Nile red) showed no photobleaching effect. Oscillations in Ca^{2+} level and mast cell degranulation were not observed without stimulation in 2 mM Ca^{2+} medium when monitored in real-time (Fig. 2A and C). However, the Ca^{2+} ionophore, Iono, could spontaneously trigger a rapid and dramatic extracellular Ca^{2+} influx, subsequently followed by mast cell degranulation (Fig. 2B and C; Supplementary videos, V1 and V2). In order to detect the increase in Ca^{2+} level in the entire cell, TIRFM was used in the wide-field mode. In contrast, the mast cell degranulation patterns were monitored using the TIRF mode, through a 65-nm optical section beneath the plasma membrane using evanescent wave imaging.

2.3. Ca^{2+} oscillation and mast cell degranulation patterns mediated by GPCR and FcεRI signaling pathways

In this study, 48/80 and TNP-BSA were used to activate GPCR- and FcεRI-mediated signaling pathways, respectively. 48/80 resulted in a five-fold increase in Ca^{2+} level, following which the Ca^{2+} level returned to basal after 5 min. Increase in the Ca^{2+} level subsequently resulted in the degranulation of mast cells (Fig. 3A and C). In contrast, TNP-BSA induced a six-fold and more sustained increase in the Ca^{2+} levels upon stimulation. The pattern of initial Ca^{2+} mobilization and of mast cell degranulation following activation with TNP-BSA was similar to that with 48/80 (Fig. 3B and C). The peak level and duration of Ca^{2+} elevation by stimulation with TNP-BSA was greater than that by 48/80 (Fig. 3C). Moreover, Ca^{2+} mobilization by activation with TNP-BSA was similar to that with Iono treatment, which immediately triggered and sustainably maintained elevated Ca^{2+} levels followed by mast cell degranulation (Figs. 2 C and 3 C). Quantitative data for different activators showed the fastest rate of mast cell degranulation ($D_{1/2}$: the time required for degranulation of fifty percent histamine after stimulation) with Iono compared to 48/80 and TNP-BSA treatments in 2 mM Ca^{2+} medium (Fig. 3D). However, there was no significant difference in the rate of mast cell degranulation between stimulation by 20 and 40 μg/mL 48/80, and 10 and 20 μg/mL TNP-BSA (Fig. 3D).

2.4. Release of Ca^{2+} from ER is both necessary and sufficient for mast cell degranulation

In order to understand whether Ca^{2+} released from the intracellular Ca^{2+} store was critical for mast cell degranulation, the cells were pretreated BAPTA-AM to load them with the intra-

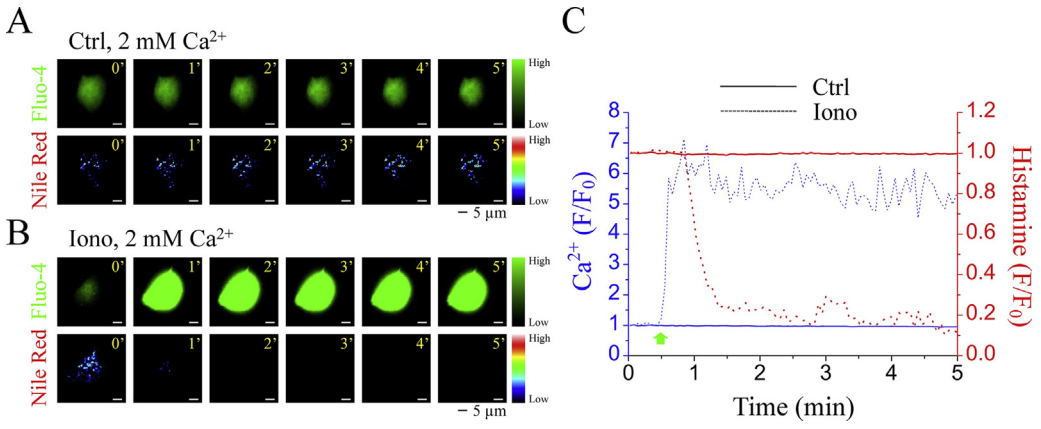

Fig. 2. Mast cell degranulation mediated by Iono-induced Ca^{2+} influx. Figure showing real-time monitoring of intracellular Ca^{2+} elevation and degranulation in RBL-2H3 mast cell using TIRFM in (A) 0.1% DMSO (Ctrl) and (B) Iono (5 μM) containing medium after pretreatment of cells with Fluo-4 AM and Nile red. Representative images depicting Ca^{2+} and histamine levels in green and pseudo-color, respectively. Cells were treated with DMSO or Iono at 30 s (scale bar, 5 μm). (C) Quantitative analyses of the relative levels of Ca^{2+} (blue) and histamine (red) in the Ctrl (solid line) and 5 μM Iono (dash line) group. The green arrow indicates Iono treatment at 30 s. (For interpretation of the references to colour in this figure legend, the reader is referred to the web version of this article.)

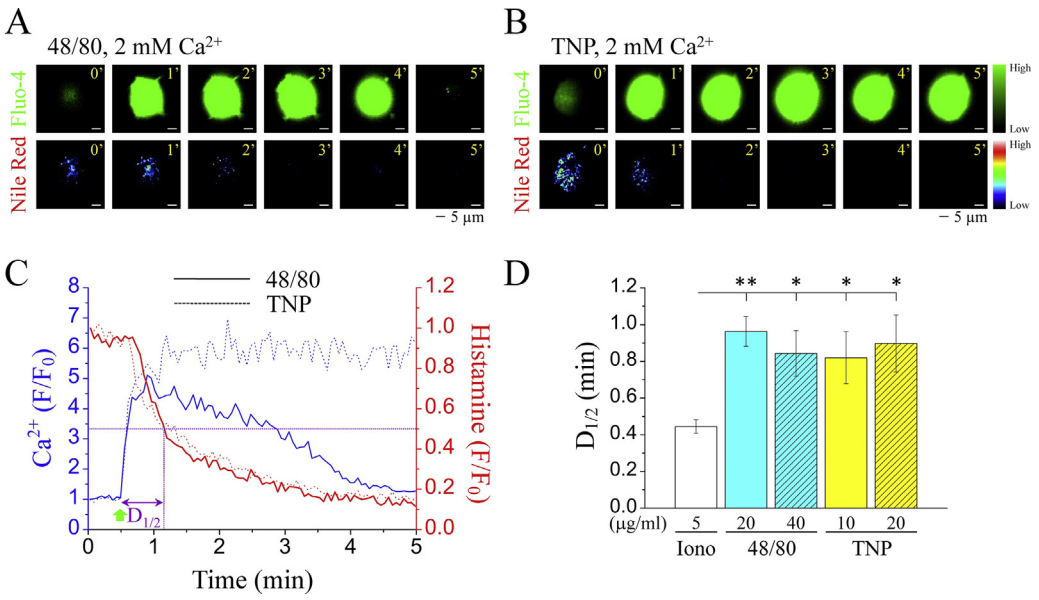

Fig. 3. Comparison of Ca^{2+} elevation and mast cell degranulation mediated by activation of GPCR and FcεRI. Figure showing real-time monitoring of intracellular Ca^{2+} elevation and degranulation using TIRFM in RBL-2H3 mast cells activated with (A) 48/80 (20 μg/mL), and (B) TNP (10 μg/mL), after pretreatment with Fluo-4 AM and Nile red in 2 mM Ca^{2+}-containing medium. 48/80 and TNP were used to activate GPCR and FcεRI, respectively. Representative images depicting Ca^{2+} and histamine levels in green and pseudo-color, respectively (scale bar, 5 μm). (C) Quantitative analyses of the relative levels of Ca^{2+} (blue) and histamine (red) in the 48/80-(solid line) and TNP (dash line)-activated group. The green arrow indicates treatment with 48/80 or TNP at 30 s, while the purple dash line indicates $D_{1/2}$. (D) Quantitative analyses of $D_{1/2}$ after 48/80 or TNP-mediated activation compared to Iono treatment in 2 mM Ca^{2+}-containing medium. All values are represented as mean ± SEM (where, n> = 10). The data were found to be statistically significant at $p < 0.05$ (indicated by *) and $p < 0.01$ (indicated by **). (For interpretation of the references to colour in this figure legend, the reader is referred to the web version of this article.)

cellular Ca^{2+} chelator (BAPTA) and later activated using different stimulators in Ca^{2+}-free medium. Data indicated no changes in Ca^{2+} level and mast cell degranulation after stimulation by 48/80 (20 μg/mL) or TNP-BSA (10 μg/mL) in BAPTA-AM-pretreated cells (Fig. 4). This indicated that Ca^{2+} signaling was necessary for mast cell degranulation. Furthermore, the cells were activated with different stimulators in the Ca^{2+}-free medium in order to differentiate between the intracellular and extracellular Ca^{2+} sources for mast cell degranulation.

The Ca^{2+} ionophore, Iono, could not trigger Ca^{2+} influx in the Ca^{2+}-free medium, and hence mast cell degranulation was not observed (Fig. S1, A and B). In contrast, 48/80 and TNP-BSA could initiate intracellular Ca^{2+} release, as a result of which mast cell degranulation subsequently occurred without the influx of extracellular Ca^{2+} (Fig. S1, C and D; Fig. 5A and B). The rate of mast cell degranulation in the Ca^{2+}-free media was slower than that in the media containing Ca^{2+} (2 mM) using different stimulators. However, 48/80 and TNP-BSA-induced increase in intracellular Ca^{2+} levels resulted in complete degranulation of mast cells even in

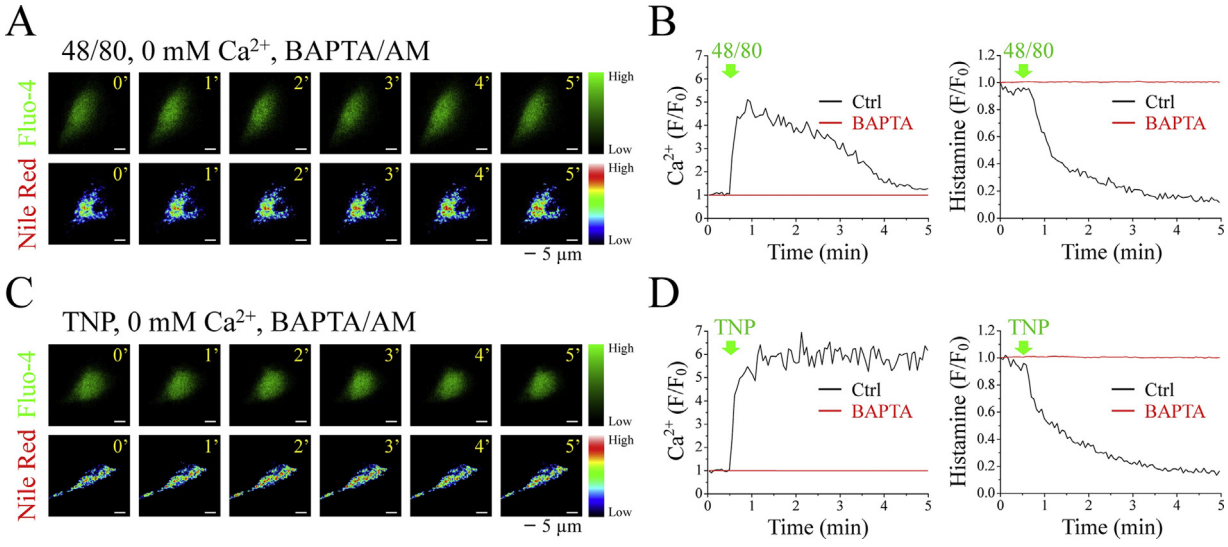

Fig. 4. Inhibition of mast cell degranulation by chelation of intracellular Ca^{2+}. Figure showing real-time monitoring of intracellular Ca^{2+} elevation and degranulation of RBL-2H3 mast cells treated with 0.1% DMSO (Ctrl) or BAPTA-AM (30 μM) and activated by (A) 48/80 (20 μg/mL), and (C) TNP (10 μg/mL) by TIRFM in Ca^{2+}-free medium (0 mM). Representative images showing Ca^{2+} and histamine levels in green and pseudo-color, respectively (scale bar, 5 μm). Quantitative analyses of the relative Ca^{2+} (left panel) and histamine (right panel) levels after stimulation by (B) 48/80 and (D) TNP. The green arrows indicate treatment with 48/80 or TNP at 30 s. (For interpretation of the references to colour in this figure legend, the reader is referred to the web version of this article.)

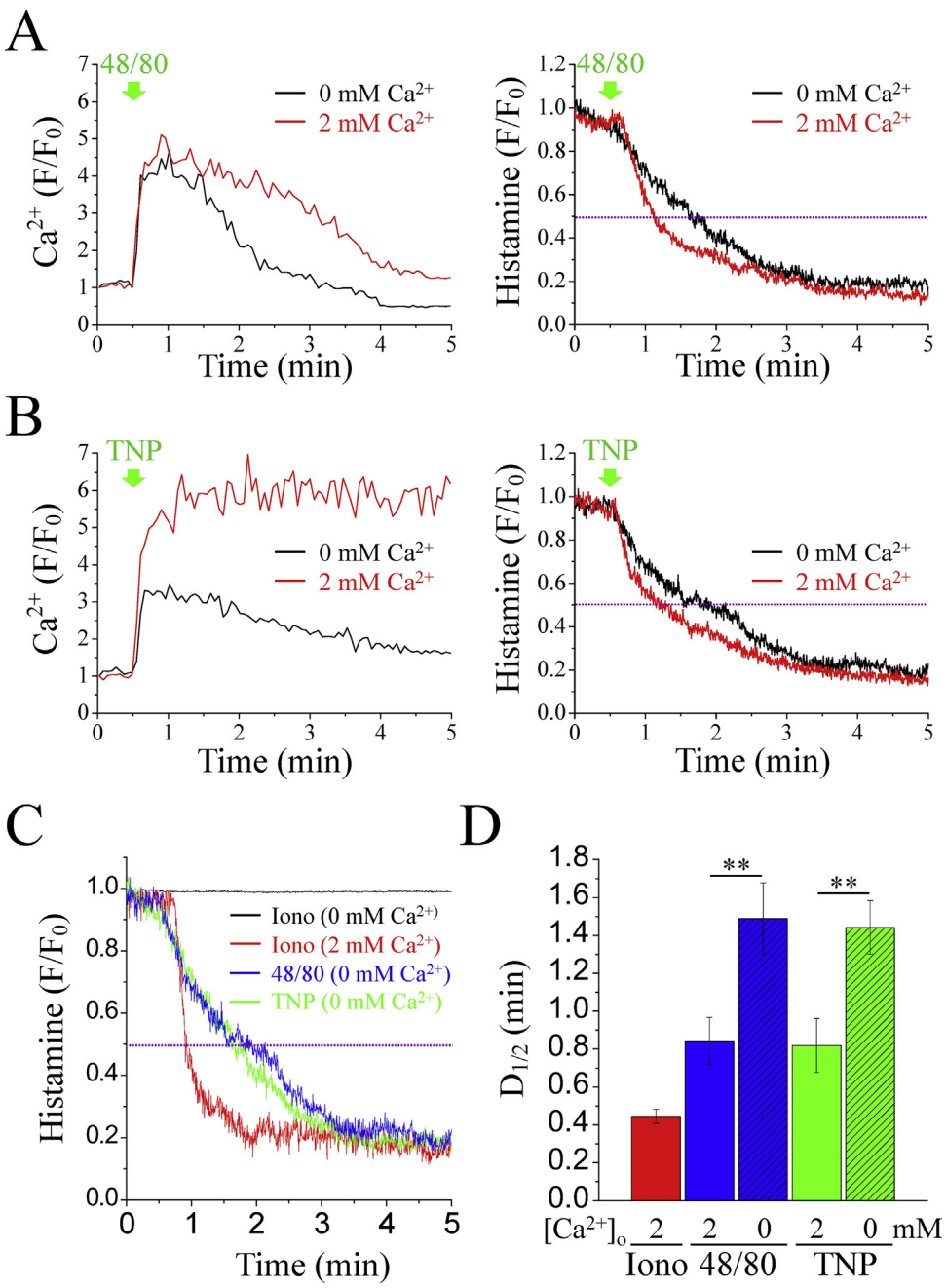

Fig. 5. Extracellular Ca^{2+} promotes but is not necessary for mast cell degranulation. Figure showing real-time monitoring of the intracellular Ca^{2+} elevation and degranulation of RBL-2H3 cells activated by (A) 48/80 (20 μg/mL) and (B) TNP (10 μg/mL) by TIRFM in Ca^{2+}-free (0 mM Ca^{2+}) or Ca^{2+}-containing (2 mM Ca^{2+}) media. Cells were pretreated with Fluo-4 AM or Nile red, and 48/80 and TNP were used to activate GPCR and FcεRI, respectively. Quantitative analyses of the relative Ca^{2+} (left panel) and histamine (right panel) levels after cells were treated with (A) or (B). The green arrows indicate 48/80 or TNP treatment at 30 s. (C) Mast cell degranulation curves of Iono, 48/80 or TNP-activated RBL-2H3 cells in 0 or 2 mM Ca^{2+} media. (D) Quantitative analyses of $D_{1/2}$ in Iono, 48/80 or TNP-activated cells in 0 or 2 mM Ca^{2+} media. All values are represented as mean ± SEM (where, n > = 10). The purple dash lines represent $D_{1/2}$. The data were found to be statistically significant at $p \leq 0.01$ (indicated by **). (For interpretation of the references to colour in this figure legend, the reader is referred to the web version of this article.)

Ca^{2+}-free media (Fig. 5A and B). Quantitative data showing the pattern and the time required for $D_{1/2}$ revealed that the rate of mast cell degranulation with different activators in Ca^{2+}-free medium was significantly slower than that by Iono in media containing Ca^{2+} (2 mM). However, Iono could not trigger mast cell degranulation in the Ca^{2+}-free medium (Fig. 5C). Furthermore, the rate of mast cell degranulation in the Ca^{2+}-free medium was significantly slower than that in the Ca^{2+}-containing (2 mM) medium using different stimulators (Fig. 5D). Thus, release of intracellular (not extracellular) Ca^{2+} alone is both essential and sufficient for mast cell degranulation. However, the rate of mast cell degranulation increases upon extracellular Ca^{2+} influx.

2.5. Delay in mast cell degranulation via downregulation of SOCE

ER is the main intracellular Ca^{2+} storage site, whereas SOCE is the major form of extracellular Ca^{2+} influx in non-excitable cells after Ca^{2+} depletion in ER [30,31]. TG, an inhibitor of the sarco/endoplasmic reticulum Ca^{2+}-ATPase (SERCA), was used to extrude Ca^{2+} from the lumen of the ER as ER-releasable Ca^{2+}, and

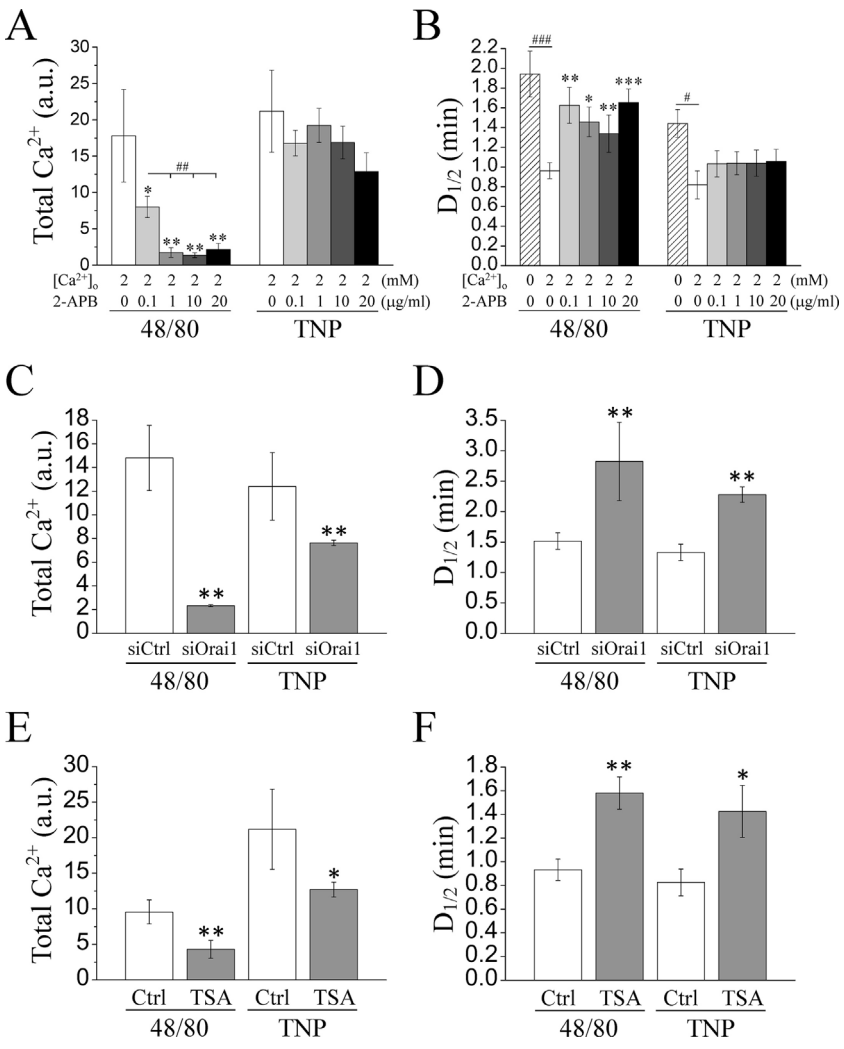

Fig. 6. Downregulation of SOCE delays mast cell degranulation. Real-time monitoring of intracellular Ca^{2+} elevation and mast cell degranulation by TIRFM for 5 min in 2 mM Ca^{2+}. Quantitative analyses of the elevation in Total Ca^{2+} (A & C & E) and $D_{1/2}$ (B & D & F) in the cells after 48/80 or TNP stimulation. Pretreatment with different concentrations of 2-APB (A & B), TSA (E & F) and knockdown of Orai1 (C & D) were used to block SOCE, before treating the RBL-2H3 mast cells with Fluo-4 AM or Nile red. 48/80 (20 μg/mL) and TNP (10 μg/mL) were used to activate GPCR and FcεRI, respectively. 0.1% DMSO was used as a control (Ctrl) of TSA. All values are represented as mean ± SEM (where, n> = 10). The data were found to be statistically significant at $p \leq 0.05$ (indicated by $^{*,\#}$), $p \leq 0.01$(indicated by $^{**,\#\#}$) and $p \leq 0.001$ (indicated by $^{***,\#\#\#}$).

the subsequent elevation in the Ca^{2+} level due to the influx from extracellular space was termed SOCE. Further, the treatment with SOCE inhibitor 2-APB, knockdown of the SOCE channel Orai1 by siRNA, or inhibition of STIM1 translocation to the plasma membrane by TSA were used to examine the role of SOCE on mast cell degranulation.

2-APB is considered as the most potent and widely used inhibitor for blocking SOCE. The cells were preincubated with or without 2-APB, and then stimulated with TG to induce the release of Ca^{2+} from the ER in order to activate SOCE with an aim to confirm the effect of SOCE on the oscillations in Ca^{2+} level and mast cell degranulation. Representative data showed an increase in the Ca^{2+} released from the ER in both the control and 2-APB pretreatment groups; however, increase in Ca^{2+} levels due to SOCE were not observed upon 2-APB pretreatment (Fig. S2, A and B). 2-APB inhibited SOCE but did not affect Ca^{2+} release from the ER (Fig. S2, B and C). In order to understand the effect of SOCE inhibition on Ca^{2+} mobilization and mast cell degranulation, the cells were preincubated with various concentrations of 2-APB, and then stimulated with 48/80 or TNP-BSA in medium containing Ca^{2+} (2 mM). Results showed decrease in cytoplasmic Ca^{2+} levels and delay in mast cell degranulation after stimulation by 48/80 in 2-APB pretreated cells (Fig. S3B; Fig. 6A and B). However, the total intracellular cytosolic Ca^{2+} levels remained sustainably elevated and the rate of mast cell degranulation did not change significantly with TNP-BSA activation (Fig. S3D; Fig. 6A and B). The efficiency of 2-APB in inhibiting the increase in intracellular Ca^{2+} level by stimulation with 48/80 was higher than that by TNP-BSA.

Additionally, transfection of cells with siOrai1 resulted in decrease in the extracellular Ca^{2+} influx by SOCE. After that, the cells were activated with 48/80 and TNP-BSA in Ca^{2+}-containing (2 mM) medium. Real-time monitoring showed that although the rises in Ca^{2+} levels were decreased by the knockdown of Orai1, they remained elevated resulting in mast cell degranulation by 48/80 or TNP-BSA stimulation (Fig. S4). Our data revealed the suppression of rises in cytosolic Ca^{2+} levels with Orai1 knockdown correlated with a significant slowing in the rates of mast cell degranulation (Fig. S4; Fig. 6C and D). Microtubule-dependent STIM1 translocation to the plasma membrane and its interaction with Orai1 is necessary for SOCE activation. HDAC6 regulates activation of STIM1-mediated SOCE. The cells were preincubated with an inhibitor (TSA) specific for HDAC6, and activated by 48/80 or TNP-BSA, in order to investigate whether the inhibition of STIM1 trafficking to the plasma membrane can influence mast cell degranulation. Similar to the

results obtained using siOrai1, it was observed that although the increase in Ca^{2+} levels was lesser upon TSA pretreatment, it was sufficiently high to induce mast cell degranulation by 48/80 and TNP-BSA. However, the elevation in total Ca^{2+} levels was significantly suppressed, and the rate of mast cell degranulation was significantly slower with TSA pretreatment followed by stimulation with 48/80 or TNP-BSA (Fig. S5; Fig. 6E and F). In summary, downregulation of SOCE attenuated the overall increase in the Ca^{2+} level. It also delayed, but could not completely abolish, mast cell degranulation upon stimulation by 48/80 or TNP-BSA (Fig. 6).

3. Discussion

Our study demonstrated that Ca^{2+}-mediated degranulation of mast cells was induced by both the IgE-FcεRI and GPCR signaling pathways, and was associated with Ca^{2+} mobilization. Previous studies have reported Ni^{2+} to act as a quencher of Nile red fluorescence [27,28]. In our study also the fluorescence of Nile red was strongly quenched by Ni^{2+} coordinated to the iminodiacetic acid moiety. When these ions were present in the secretory granules containing histamine, they preferably coordinated with histamine. Thereafter, the ability of Ni^{2+} to quench the fluorescence decreased, and the emission from Nile red increased drastically. Hence, we demonstrated that Nile red could be used as an effective probe for the real-time monitoring of histamine in the living cells (Fig. 1).

Ca^{2+} plays an important role in fusion of the secretory granules with the plasma membrane during exocytosis of the mast cells. We demonstrated that mast cell degranulation immediately follows Iono-mediated Ca^{2+} elevation (Fig. 2). Elevation in the intracellular Ca^{2+} level after stimulation by allergens may be attributed to the ER-releasable Ca^{2+} and the extracellular Ca^{2+} influx through IgE-FcεRI or GPCR-mediated signaling. TNP-BSA and 48/80 were used to differentiate between the effect of IgE-FcεRI and GPCR-mediated signaling on Ca^{2+} mobilization and mast cell degranulation, respectively. The increase in Ca^{2+} level by stimulation with TNP-BSA was higher and more sustained than that by 48/80. However, there was no significant difference in the mast cell degranulation rate upon stimulation by both these compounds. Both, IgE-FcεRI and GPCR-mediated mast cell degranulation occurred after 5–6 fold elevation in cytosolic Ca^{2+} levels in the medium, respectively (Fig. 3). A previous study has reported the threshold of Ca^{2+} elevation for mast cell degranulation as 200 nM [32], which is twice the resting Ca^{2+} concentration (~100 nM). This indicates that even a small increase in the Ca^{2+} levels is sufficient for mast cell degranulation and histamine release.

We also studied the importance of intracellular Ca^{2+} release and extracellular Ca^{2+} influx on mast cell degranulation. TNP-BSA and 48/80 induced intracellular Ca^{2+} elevation and mast cell degranulation in cells cultured in Ca^{2+}-free medium, however the Ca^{2+} level and mast cell degranulation rate were lesser compared to the cells cultured in normal medium (2 mM Ca^{2+}). There was no significant difference in the capacity of mast cell degranulation (Fig. 5A and B). When the Ca^{2+} levels increased to the threshold value, it was sufficient to cause mast cell degranulation. However, no increase in the Ca^{2+} level or mast cell degranulation were observed after stimulation by TNP-BSA or 48/80 in Ca^{2+}-free medium, when cells were pretreated with the intracellular Ca^{2+} chelator BAPTA (Fig. 4). These results indicated that the elevation in Ca^{2+} level mediated by its release from the ER was sufficient for inducing mast cell degranulation, even though the extracellular Ca^{2+} influx was not operational. However, the rate of mast cell degranulation was significantly higher under conditions of extracellular Ca^{2+} influx in normal medium. Therefore, we proved that intracellular Ca^{2+} was both necessary and sufficient for mast cell degranulation; however, extracellular Ca^{2+} influx enhanced the process as evident by shorter $D_{1/2}$ values (Fig. 5D). In addition, Ca^{2+} increase in the center of the cell was found to be higher than that in the periphery, as observed by activation with TNP-BSA or 48/80 in Ca^{2+}-free medium (Fig. S5). We found that 48/80 induced intracellular Ca^{2+} elevation in the central region followed by the extracellular influx in the peripheral region (Fig. S5, A and C). In contrast, TNP-BSA induced rapid intracellular Ca^{2+} elevation in both central and peripheral regions in 2 mM Ca^{2+} medium. In addition, Ca^{2+} increase in the center of the cell was found to be higher than that in the periphery, as observed by activation with TNP-BSA or 48/80 in Ca^{2+}-free medium (Fig. S5A). This may be due to the depletion of Ca^{2+} from the ER and absence of extracellular Ca^{2+} influx in the Ca^{2+}-free medium. In comparison to 48/80 stimulation in Ca^{2+}-free medium, Ca^{2+} elevation induced by TNP-BSA was decreased more rapidly and dramatically (Fig. S6A). It indicates that extracellular Ca^{2+} influx is a major contributing factor to the elevation of intracellular Ca^{2+} after TNP-BSA stimulation compared to 48/80 stimulation. This observation can also be confirmed in Fig. 5A and B that TNP-BSA-induced intracellular Ca^{2+} elevation was significantly decreased in the Ca^{2+}-free medium.

Several reports have revealed diverse physiological functions for cells involved in massive Ca^{2+} influx, including osteogenesis [33], activation of effector T-cells [34], macrophage-mediated inflammasome activation [35], dendritic cell maturation [36], antigen presentation [37], inflammation [38], stem cell differentiation [39], and cancer metastasis [40]. Here, we investigated the role of SOCE in the regulation of mast cell degranulation. The cytosolic Ca^{2+} levels were significantly reduced, and the rate of mast cell degranulation was significantly lesser as a result of 2-APB pretreatment and 48/80 stimulation (Fig. 6; Fig. S3). However, both the parameters were not significantly affected upon TNP-BSA stimulation (Fig. 6; Fig. S3). This may be due to the fact that TNP-BSA initially triggers a large increase in the Ca^{2+} levels, which is sufficient for mast cell degranulation. In this study, Orai1 knockdown and TSA pretreatment were also used to inhibit SOCE. While Orai1 is the main channel for mediating SOCE, TSA inhibits STIM1 trafficking to the plasma membrane through the microtubules [41]. The cytosolic Ca^{2+} levels decreased and the rate of mast cell degranulation became significantly slower as a result of Orai1 knockdown and TSA pretreatment, similar to the stimulation with TNP-BSA and 48/80 (Fig. 6; Figs. S4 and S5). These results support that the extracellular Ca^{2+} influx promotes mast cell degranulation.

The acute and chronic inflammatory reactions triggered by mast-cell activation have important pathophysiological consequences in allergy, which may depend on the dose of antigen and its route of entry. The IgE-FcεRI complex and mast cells have been convincingly linked to many acute hypersensitive and allergic reactions, such as acute asthma, anaphylactic shock, atopic dermatitis, coronary inflammation, and inflammatory arthritis [42–44]. Whereas, cationic amphipathic peptides, including mast cell degranulating peptide, neuropeptides, and the synthetic histamine releaser compound 48/80 act on GPCR may associate with chronic allergic inflammation and other allergic disorders, such as chronic asthma, urticaria, itch and neurogenic inflammation [45–47]. It was also reported that mast cells can release granule matrix materials slowly or more rapidly. GPCR typically activate transient Ca^{2+} responses in mast cells. In this study, we found that FcεRI-induced Ca^{2+} increase was higher and more sustained than that induced by GPCR. The biological significance of the differences between FcεRI- and GPCR pathways can be explained by the fact that FcεRI produced a rapid and strong activation for histamine degranulation, resulting in most acute allergic reactions. On the other hand, GPCR produced a moderate and prolong activation for histamine degranulation, resulting in major chronic allergic inflammation. Similar to the activation of PLCγ by the IgE-FcεRI complexes, activation of PLCβ by GPCRs also leads to the hydrolysis

of PIP2 to yield DAG and IP_3. The common secondary messengers, DAG and IP_3, are produced to relay signal and exert an influence in response to the activation of FcεRI and GPCR. We proposed that the different responses of Ca^{2+} elevation and histamnie degranulation to TNP-BSA and compound 48/80 stimulation are determined mainly by the strength and frequency of the PLCs-DAG/IP_3 axis. TNP-BSA stimulation produces a rapid and strong PLCγ- DAG/IP_3 activation, resulting in a large Ca^{2+} influx following ER Ca^{2+} release. In compared to TNP-BSA stimulation, compound 48/80 may exert a moderate and prolonged PLCβ-DAG/IP_3 activation, resulting in a moderate Ca^{2+} influx following persistent ER Ca^{2+} release (Fig. 5A and B; Fig. S6).

In this study, we examined Ca^{2+} mobilization and mast cell degranulation with different stimulators to understand the differences between the FcεRI- and GPCR-mediated signaling. We concluded that even though intracellular Ca^{2+} release by ER was both necessary and sufficient for mast cell degranulation in both the pathways, influx of extracellular Ca^{2+} augmented the process. This was supported by the decrease in mast cell degranulation observed upon downregulation of SOCE. Based on our results, we further propose that this can be developed as a model system to screen drugs for allergic diseases in the future.

4. Materials and methods

4.1. Cell culture maintenance and transfection

The rat basophilic leukemia (RBL-2H3) cell line was maintained in high glucose Dulbecco's modified Eagle's medium (DMEM; GIBCO, Big Cabin, OK, USA) supplemented with 10% fetal bovine serum (FBS; GIBCO, Big Cabin, OK, USA), penicillin (100 IU/mL), and streptomycin (100 μg/mL) in 5% CO_2 at 37 °C. For transient transfection, the CD63-GFP plasmid construct, scrambled siRNA (siCtrl) and Orai1 siRNA (siOrai1) were transfected into RBL-2H3 cells using Lipofectamine 3000 (Invitrogen, San Diego, CA, USA) for 48 h. The rat siOrai1 target sequence, 5′-CAACAGCAAUCCGGAGCUU-3′ (sense strand) and 5′-AAGCUCCGGAUUGCUGUUG-3′ (antisense strand) [48]; and the siCtrl sequence, 5′-UAAGGCUAUGAAGAGAUAC-3′ (sense strand) and 5′-GUAUCUCUUCAUAGCCUUA-3′ (antisense strand), were purchased from Invitrogen (San Diego, CA, USA).

4.2. Chemical reagents

Ionomycin (Iono), 2-APB, BAPTA-AM, Nile red, $NiCl_2$, thapsigargin (TG) and tubastatin A (TSA) were purchased from Sigma-Aldrich (Saint Louis, MO, USA). Fluo-4 AM, trinitrophenyl-bovine serum albumin (TNP-BSA) and anti-TNP monoclonal antibody were purchased from Invitrogen (San Diego, CA, USA), Santa Cruz Biotechnology (Santa Cruz, CA, USA), and BD Pharmingen (San Diego, CA, USA), respectively.

4.3. Measurement of ER-releasable Ca^{2+} and SOCE

The intracellular Ca^{2+} concentration was measured using TIRFM (cellTIRF; Olympus, Tokyo, Japan) in the wide-field mode, to understand the global changes occurring in the cytosolic Ca^{2+} levels in the mast cells. Intracellular Ca^{2+} was measured at 37 °C using the fluorescent Ca^{2+} indicator Fluo-4. Cells were seeded at a density of 5×10^4 cells in a 3 cm glass-bottomed culture dish, and incubated with Fluo-4 AM (2 μM) for 30 min. Ca^{2+} release from the ER (ER-releasable Ca^{2+}) was induced by the addition of TG (2 μM) for 10 min in Ca^{2+}-free buffer. Thereafter, Ca^{2+} influx by SOCE was triggered by exchange with extracellular Ca^{2+} buffers (0–2 mM) for 5 min at time point "10 min". Images were collected at 3-s intervals for 5 min.

4.4. Measurement of Ca^{2+} mobilization and mast cell degranulation

To mimic physiological stimulation, cells were seeded at a density of 5×10^4 cells in a 3 cm glass-bottomed dish overnight, and incubated with 0.2 μg/mL monoclonal anti-TNP IgE antibody (anti-TNP IgE) for 4 h at 37 °C. The IgE-sensitized cells were washed three times with PBS to remove any unbound anti-TNP IgE. The cells were treated with Ca^{2+} indicator Fluo-4 (2 μM) and Nile red (1 μM) after preincubating with Ni^{2+} (100 μM) in the culture medium for 30 min at 37 °C. For Ca^{2+} and histamine measurements, the cells were activated with 10 and 20 μg/mL TNP-BSA in phenol red-free medium (GIBCO, Big Cabin, OK, USA) for 5 min and observed using TIRFM (cellTIRF; Olympus, Tokyo, Japan). For understanding the basic secretagogue-mediated signaling pathway, the cells were activated with 20 and 40 μg/mL of 48/80 in phenol red-free medium. Fluo-4 was excited using a mercury lamp under the wild-field mode to record the global oscillations in the cytosolic Ca^{2+} levels, whereas Nile red was excited using laser (561 nm) under the TIRF mode to observe mast cell degranulation near the plasma membrane. The pattern of Ca^{2+} oscillations and mast cell degranulation were acquired from the images obtained using a cooled charge-coupled device (CCD) camera controlled by the Xcellence software (Olympus, Tokyo, Japan) at intervals of 3 s per frame. Quantification of mast cell degranulation was performed by determining the time required for degranulation of fifty percent histamine ($D_{1/2}$) after stimulation, whereas Ca^{2+} levels were calculated based on the area under the curve.

4.5. Immunofluorescence and confocal microscopy

The cells overexpressing CD63-GFP were fixed in paraformaldehyde (4%), permeabilized with Triton X-100 (0.5%) for 15 min, and washed three times with PBS. The fixed cells prepared earlier were blocked with CAS-Block (Invitrogen, Carlsbad, CA, USA) at 25 °C for 1 h. They were incubated with primary anti-histamine antibody (Abcam, San Francisco, CA, USA) overnight at 4 °C. Unbound antibody was removed by washing with PBS five times, following which the cells were incubated with Alexa fluor 543-conjugated secondary antibody (Invitrogen, Carlsbad, CA, USA) for 1 h. The unbound antibody was removed by washing with PBS five times, and images were obtained using excitation wavelengths of 488 nm or 543 nm under a confocal microscope.

4.6. Statistical analysis

Data were represented as mean ± SEM (standard error of mean). Student's *t*-test was used to calculate significant differences between different data groups, where $p < 0.05$ was considered to be statistically significant.

Conflicts of interest

The authors declare that they have no conflicts of interest.

Acknowledgements

We thank Dr. Juan S. Bonifacino (NIH, MD) for kindly providing the CD63-GFP plasmid construct and Dr. Lung-Sen Kao (National Yang-Ming University, Taiwan) for providing technical support. We also thank the "Bio-image Core Facility of the National Core Facility Program for Biotechnology, Ministry of Science and Technology,

Taiwan" for their technical services. We acknowledge the financial support provided by the Ministry of Science and Technology of Taiwan under Grant No. MOST 105-2633-B-006-002 and 105-2628-B-006-003-MY3.

Appendix A. Supplementary data

Supplementary data associated with this article can be found, in the online version, at http://dx.doi.org/10.1016/j.ceca.2017.08.002.

References

[1] S.M. Miescher, M. Vogel, Molecular aspects of allergy, Mol. Aspects Med. 23 (2002) 413–462.
[2] A.M. Gilfillan, M.A. Beaven, Regulation of mast cell responses in health and disease, Crit. Rev. Immunol. 31 (2011) 475–529.
[3] S. Odom, T. Yamashita, A.M. Gilfillan, et al., Cutting edge: genetic variation influences FcεRI-induced mast cell activation and allergic responses, J. Immunol. 179 (2007) 740–743.
[4] M. Aridor, L.M. Traub, R. Sagi-Eisenberg, Exocytosis in mast cells by basic secretagogues: evidence for direct activation of GTP-binding proteins, J.Cell Biol. 111 (1990) 909–917.
[5] U. Blank, J. Rivera, The ins and outs of IgE-dependent mast-cell exocytosis, Trends Immunol. 25 (2004) 266–273.
[6] R. Cohen, A. Torres, H.T. Ma, D. Holowka, B. Baird, Ca^{2+} waves initiate antigen-stimulated Ca^{2+} responses in mast cells, J. Immunol. 183 (2009) 6478–6488.
[7] D. Holowka, N. Calloway, R. Cohen, et al., Roles for Ca^{2+} mobilization and its regulation in mast cell functions, Front. Immunol. 3 (2012) 104.
[8] D. Holowka, D. Sil, C. Torigoe, B. Baird, Insights into immunoglobulin E receptor signaling from structurally defined ligands, Immunol. Rev. 217 (2007) 269–279.
[9] J.L. Bueb, M. Mousli, Y. Landry, Molecular basis for cellular effects of naturally occurring polyamines, Agents Actions 33 (1991) 84–87.
[10] A.M. Rothschild, Mechanisms of histamine release by compound 48–80, Br. J. Pharmacol. 38 (1970) 253–262.
[11] M. Mousli, C. Bronner, J.L. Bueb, E. Tschirhart, J.P. Gies, Y. Landry, Activation of rat peritoneal mast cells by substance P and mastoparan, J. Pharmacol. Exp. Ther. 250 (1989) 329–3358.
[12] X. Ferry, V. Eichwald, L. Daeffler, Y. Landry, Activation of βγ subunits of G_{i2} and G_{i3} proteins by basic secretagogues induces exocytosis through phospholipase Cβ and arachidonate release through phospholipase Cγ in mast cells, J. Immunol. 167 (2001) 4805–4813.
[13] J.L. Bueb, M. Mousli, C. Bronner, B. Rouot, Y. Landry, Activation of G_i-like proteins, a receptor-independent effect of kinins in mast cells, Mol. Pharm. 38 (1990) 816–822.
[14] H. Ali, Regulation of human mast cell and basophil function by anaphylatoxins C3a and C5a, Immunol. Lett. 128 (2010) 36–45.
[15] X. Ferry, S. Brehin, R. Kamel, Y. Landry, G protein-dependent activation of mast cell by peptides and basic secretagogues, Peptides 23 (2002) 1507–1515.
[16] R.T. Dorsam, J.S. Gutkind, G-protein-coupled receptors and cancer, Nat. Rev. Cancer 7 (2007) 79–94.
[17] C.C. Huang, D.M. Yang, C.C. Lin, L.S. Kao, Involvement of Rab3A in vesicle priming during exocytosis: interaction with Munc13-1 and Munc18-1, Traffic 12 (2011) 1356–1370.
[18] U. Blank, I.K. Madera-Salcedo, L. Danelli, et al., Vesicular trafficking and signaling for cytokine and chemokine secretion in mast cells, Front. Immunol. 5 (2014) 453.
[19] T.D. Kim, G.T. Eddlestone, S.F. Mahmoud, J. Kuchtey, C. Fewtrell, Correlating Ca^{2+} responses and secretion in individual RBL-2H3 mucosal mast cells, J. Biol. Chem. 272 (1997) 31225–31229.
[20] R. Cohen, K. Corwith, D. Holowka, B. Baird, Spatiotemporal resolution of mast cell granule exocytosis reveals correlation with Ca^{2+} wave initiation, J. Cell Sci. 125 (2012) 2986–2994.
[21] Y. Tojyo, T. Morita, A. Nezu, A. Tanimura, Key components of store-operated Ca^{2+} entry in non-excitable cells, J. Pharmacol. Sci. 125 (2014) 340–346.
[22] A.J. Smith, J.R. Pfeiffer, J. Zhang, A.M. Martinez, G.M. Griffiths, B.S. Wilson, Microtubule-dependent transport of secretory vesicles in RBL-2H3 cells, Traffic 4 (2003) 302–312.
[23] S. Nishida, et al., FcεRI-mediated mast cell degranulation requires calcium-independent microtubule-dependent translocation of granules to the plasma membrane, J. Cell Biol. 170 (2005) 115–126.
[24] J. Di Capite, A.B. Parekh, CRAC channels and Ca^{2+} signaling in mast cells, Immunol. Rev. 231 (2009) 45–489.
[25] M. Vig, J.P. Kinet, Calcium signaling in immune cells, Nat. Immunol. 101 (2009) 21–27.
[26] R. Suzuki, X. Liu, A. Olivera, et al., Loss of TRPC1-mediated Ca^{2+} influx contributes to impaired degranulation in Fyn-deficient mouse bone marrow-derived mast cells, J. Leukoc. Biol. 88 (2010) 863–875.
[27] D. Seto, N. Soh, K. Nakano, T. Imato, An amphiphilic fluorescent probe for the visualization of histamine in living cells, Bioorg. Med. Chem. Lett. 20 (2010) 67085–67110.
[28] D. Seto, N. Soh, K. Nakano, T. Imato, Selective fluorescence detection of histamine based on ligand exchange mechanism and its application to biomonitoring, Anal. Biochem. 404 (2010) 135–139.
[29] T.D. Kim, G.T. Eddlestone, S.F. Mahmoud, et al., Correlating Ca^{2+} responses and secretion in individual RBL-2H3 mucosal mast cells, J. Biol. Chem. 272 (1997) 31225–31229.
[30] T. Hewavitharana, X. Deng, J. Soboloff, D.L. Gill, Role of STIM and Orai proteins in the store-operated calcium signaling pathway, Cell Calcium 42 (2007) 173–182.
[31] Y. Tojyo, T. Morita, A. Nezu, A. Tanimura, Key components of store-operated Ca^{2+} entry in non-excitable cells, J. Pharmacol. Sci. 125 (2014) 340–346.
[32] J. Senyshyn, R.A. Baumgartner, M.A. Beaven, Quercetin sensitizes RBL-2H3 cells to polybasic mast cell secretagogues through increased expression of G_i GTP-binding proteins linked to a phospholipase C signaling pathway, J. Immunol. 160 (1998) 5136–5144.
[33] M.W. Grol, I. Zelner, S.J. Dixon, $P2X_7$-mediated calcium influx triggers a sustained, PI3K-dependent increase in metabolic acid production by osteoblast-like cells, Am. J. Physiol. Endocrinol. Metab. 302 (2012) E561–E575.
[34] N. Joseph, B. Reicher, M. Barda-Saad, The calcium feedback loop and T cell activation: how cytoskeleton networks control intracellular calcium flux, Biochim. Biophys. Acta 1838 (2014) 557–568.
[35] J.R. Yaron, S. Gangaraju, M.Y. Rao, et al., K^+ regulates Ca^{2+} to drive inflammasome signaling: dynamic visualization of ion flux in live cells, Cell. Death. Dis. 6 (2015) e1954.
[36] R. Félix, D. Crottès, A. Delalande, et al., The Orai-1 and STIM-1 complex controls human dendritic cell maturation, PLoS One 8 (2013) e61595.
[37] M.I. Lioudyno, J.A. Kozak, A. Penna, et al., Orai1 and STIM1 move to the immunological synapse and are up-regulated during T cell activation, Proc. Natl. Acad. Sci. U. S. A. 105 (2008) 2011–2016.
[38] W.C. Chang, Store-operated calcium channels and pro-inflammatory signals, Acta Pharmacol. Sinl. 27 (2006) 813–820.
[39] T.J. Kim, J. Sun, S. Lu, Y.X. Qi, Y. Wang, Prolonged mechanical stretch initiates intracellular calcium oscillations in human mesenchymal stem cells, PLoS One 9 (2014) e109378.
[40] N. Prevarskaya, R. Skryma, Y. Shuba, Calcium in tumour metastasis: new roles for known actors, Nat. Rev. Cancer 11 (2011) 609–618.
[41] Y.T. Chen, Y.F. Chen, W.T. Chiu, et al., Microtubule-associated histone deacetylase 6 supports the calcium store sensor STIM1 in mediating malignant cell behaviors, Cancer Res. 73 (2013) 4500–4509.
[42] C.M. Williams, S.J. Galli, The diverse potential effector and immunoregulatory roles of mast cells in allergic disease, J. Allergy Clin. Immunol. 105 (2000) 847–859.
[43] T.C. Theoharides, D. Kalogeromitros, The critical role of mast cells in allergy and inflammation, Ann. N. Y. Acad. Sci. 1088 (2006) 78–99.
[44] S.J. Galli, M. Tsai, IgE and mast cells in allergic disease, Nat. Med. 18 (2012) 693–704.
[45] Y. Okayama, H. Saito, C. Ra, Targeting human mast cells expressing g-protein-coupled receptors in allergic diseases, Allergol. Int. 57 (2008) 197–203.
[46] P. Zhao, T. Hiramoto, Y. Asano, C. Kubo, N. Sudo, Chronic psychological stress exaggerates the compound 48/80-induced scratching behavior of mice, Pharmacol. Biochem. Behav. 105 (2013) 173–176.
[47] H. Subramanian, K. Gupta, H. Ali, Roles of Mas-related G protein-coupled receptor X2 on mast cell-mediated host defense pseudoallergic drug reactions, and chronic inflammatory diseases, J. Allergy Clin. Immunol. 138 (2016) 700–710.
[48] M. Potier, J.C. Gonzalez, R.K. Motiani, et al., Evidence for STIM1- and Orai1-dependent store-operated calcium influx through I_{CRAC} in vascular smooth muscle cells: role in proliferation and migration, FASEB J. 23 (2009) 2425–2437.